

# INTERNATIONAL SOCIETY FOR SOIL MECHANICS AND GEOTECHNICAL ENGINEERING



*This paper was downloaded from the Online Library of the International Society for Soil Mechanics and Geotechnical Engineering (ISSMGE). The library is available here:*

<https://www.issmge.org/publications/online-library>

*This is an open-access database that archives thousands of papers published under the Auspices of the ISSMGE and maintained by the Innovation and Development Committee of ISSMGE.*

# Ground motion site amplification factors for deep soil deposits sites in Indo- Gangetic Basin



Ketan Bajaj, Panjamani Anbazhagan  
*Indian Institute of Science, Bangalore, Karnataka, India*

## ABSTRACT

The high level of seismicity associated with the Himalayan tectonic province results in the site amplification of the deep Indo-Gangetic Basin (IGB) alluvial deposits. IGB had experienced catastrophic earthquake damages due to the presence of thick soil depth of 0.05 km to about 4 km. However, very few studies have been carried out to characterize the IGB soil up to shallow depth and limited attempts have been made to measure the dynamic properties of the deep soil column. Hence, in this study, shear velocity profile ( $V_s$ ) up to 200 m depth is measured using combined active and passive multichannel analysis of surface wave (MASW) survey in 75 selected locations in IGB. Further, these sites are classified and characterized based on time-averaged  $V_s$  in the upper 30 m depth as per NEHRP seismic site classification. The measured  $V_s$  profiles are further used to estimate the site-specific response parameters at different locations by carrying out non-linear site response analysis. Input ground motions (GMs) are selected from the worldwide-recorded database based on the seismicity of the region. Recorded GMs used in this study are taken from both global as well as local Indian network. The first time, representative site response for deep soil column and amplification factors for the different periods are estimated for IGB. Finally, the study presents the site amplification factor for different seismic site class, which would be further useful in developing a new ground motion equation considering the site amplification model and design response spectra for deep deposits in India.

## 1 INTRODUCTION

Local site conditions have great influence on ground surface motion and structural damage caused by any earthquake event. Two classic examples that emphasize the influence of site amplification due to local site effect are 1985 Mexico earthquake and the 1989 Loma Prieta earthquake. Similarly, many earthquakes in India (1934 Bihar-Nepal; 2001, Bhuj; 2015 Nepal earthquake) have also illustrated the local site effect.

The Indian subcontinent is one of the most seismically active regions in the world. The ongoing collision between the Indian and Eurasian Plate building the strain along and within the plate boundary. Moreover, crustal shortening along its northern edge increases the earthquake hazard, particularly in the Northern part Indian Subcontinent. Various authors (Bilham, 2005; 2001) have studied the seismotectonic of the Himalayan region and predicted the high seismicity along the entire stretch of the Main Boundary thrust (MBT), the Main Central thrust (MCT) and Indus-Tsangpo Suture (ITS).

In the last two centuries, the Himalayan region has experienced many events of magnitude more than 8. The highly fertile and deep basin of Indo-Gangetic Basin (IGB), bound on the north side of the Himalayas, is one of the most populous areas. It is about 1000 km long to the south is filled-up in the form of loose soil deposits. Additionally, surrounded by high seismic region make the scenario more destructive and may result in casualties to human life or infrastructure from any large earthquake in the future. Hence, there is a need to study the local site effect due to deep deposits in IGB contiguous with high seismic region. The poor characterization of deep soil deposits in IGB also set the priority for determination of its

seismic site classification and amplification factor for different periods due to local site effect.

Various authors (Boominathan et al., 2008; Anbazhagan and Sitharam, 2008; Anbazhagan et al., 2010; Kumar et al., 2012; Desai and Choudhury, 2014, 2015; Kumar et al., 2016) in India have attempted to estimate the local site effect. However, most the earlier studies were either preliminary studies or guidelines for performing site response studies. Moreover, very few studies estimated the local site effects for IGB. Anbazhagan et al. (2011) performed the site response analysis for limited sites at Dehradun, Lalru and Najibabad based on the collected borehole data and using synthetic ground motion for 1999 Chamoli EQ. Kumar et al. (2012) performed the site response analysis for typical sites at Lucknow using synthetic and recorded ground motions. Kumar et al. (2016) performed the site response study for Delhi region using the equivalent linear model. Most of the previous studies are limited to soil column of 30 m depth, additionally, in many of the studies, measured SPT-N values were converted to  $V_s$  profiles and used for site response studies. Moreover, in the previous site response studies, the input ground motions were either selected randomly from global database or simulated based on the occurred earthquake scenario. Till today there are no studies available for determining the local site effect for the deep deposits of IGB from the measured  $V_s$  profiles more than 100 m.

The first aim of the study is to develop the shear velocity ( $V_s$ ) profile up to 200 m depth using combined active and passive multichannel analysis of surface wave (MASW) survey for deep deposits in Indo-Gangetic Basin (IGB), India. In this study, geophone of 2 Hz frequency has been used for performing the MASW survey. Ambient noise has been used as a source for both passive remote

and roadside survey. Recordings have been done at different sampling interval and record lengths. Measurements are performed at different locations in the entire stretch of IGB, stretching across the Indian states from Bihar to Punjab. The sites are classified and characterized based on time-averaged  $V_s$  in the upper 30 m depth as per NEHRP (BSSC, 2003) seismic site classification.

Secondly, non-linear site response analysis has been carried out. Site response study focuses on estimation of the site amplification for deep deposits and development of a model for nonlinear soil response for possible use of ground motion developers. The input ground motions are selected based on seismicity of the region by considering global and locally available recorded ground motions. Finally, the site amplification factor has been given for different seismic site class, which would be further useful in developing new ground motion considering site amplification model and design response spectra for deep deposits in India.

## 2 STUDY AREA

The Indo-Gangetic Plain is well known as the Himalayan fore-deep lies in between the Indian Shield and the Himalayas. The Ganga Plain extends from Aravalli-Delhi Ridge in the west to the Rajmahal hills in the east; Himalayan foothills in the north to the Bundelkhand-Vindhyan Plateau in the south, occupying an area around 250,000 km<sup>2</sup>, roughly between longitude 77°E, and 88°E and latitude 24°N and 30°N. The length of the Ganga plain is about 1000 km; the width is variable, ranging from 200 to 450 km, being wider in the western part and narrower in the eastern part. Figure 1 shows the boundary of the study area considered in our study. The region has an average population > 600 million (as per 2011 census) and encompasses densely populated cities like Delhi, Lucknow, Faizabad, Kanpur, Meerut, Agra, Allahabad, and Patna.

A strong asymmetry is shown in thickness of the foreland basin of the IGB. Northwards the thickness of sediments is around 3-4 km near the Siwalik Hills. The maximum estimated thickness of sediment in the Siwalik belt is about 6-8 km. Southwards of IGB has a thickness of sediments around 0.5 to 1.0 km, it changes to around 2-2.5 in the eastern part of the IGD (See Figure 1 (a)). The detail contour of the thickness of the IGB is available in Singh, 1996. Even Singh (1996) concluded that throughout the IGB, the top few meters of the succession show a distinctive fining upward sequence, mostly terminating in mud rich sediments. The Himalaya derived gravel beds are present in the Bhabar and Terai belt; the gravel horizons of central and Alluvial plain reworked Kaankar and carbonated-cemented sand. The gravel in the southern part is derived from peninsular craton.

Additionally, the Indo-Gangetic Basin that runs parallel to the seismically active Himalayan Belt is under high risk of seismic hazard. Apart from the seismicity of the Himalayan Belt, the floor of the Gangetic trough is corrugated by inequalities and buried ridges. The geophysical information regarding the Ganga Basin shows the distinct features of the basement rock. The

metamorphic basement reveals a number of ridges and basins for which the thickness of sediments are highly variable (Singh, 1996). The important basement highs are the Delhi-Hardwar ridge, the Faizabad ridge, the Monghyr-Saharsa ridge, a poorly developed high in Mirzapur-Ghazipur area; and smaller highs of Raxaul, Bahraich and Parapur (Singh, 1966). The southern part of the Ganga Plain in Mirzapur shows E-W and ENE-WSW trending linear magnetic anomaly zones. Seismic studies in Ganga Plains indicate that the basin and ridges were also active during deposition of Late Proterozoic sediments. The vertical upliftment along the Delhi-Hardwar ridge results in incision of major drainages in the western part of the Ganga Basin. Rao (1973) recognized E-W and ENE-ESW trending active lineaments in the eastern part of the Ganga basin (See Figure 1). In this region, there are a number of E-W trending gravity faults, running parallel to the Ganga region within the narrow zone.

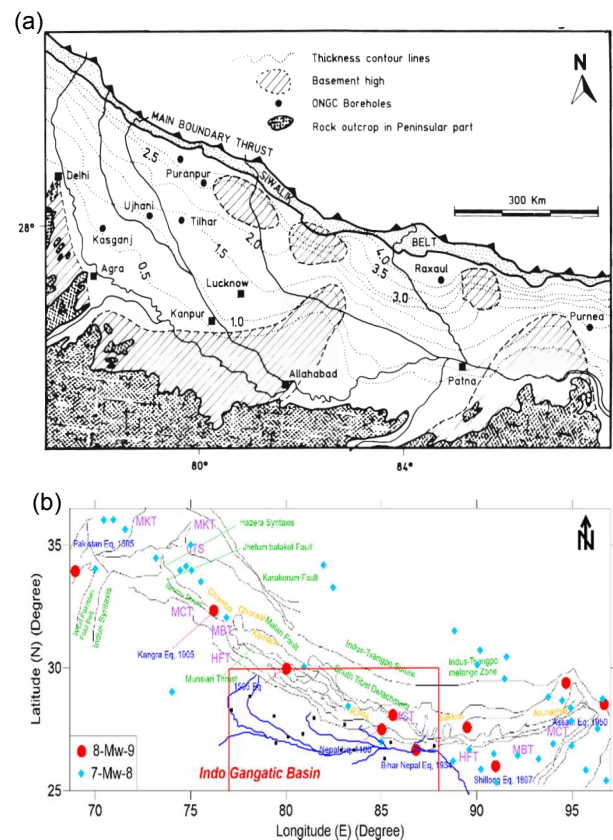


Figure 1:- (a) Contours of sediment thickness of the IGB (Taken from Singh, 1996) and (b) seismotectonic of the adjacent Himalayan region along with IGB

Gupta (2006) described the Indo-Gangetic basin as moderately active when compared to the Himalayas, and considered strike slip faults to be the major cause of earthquakes in the region. Figure 1 (b) also shows major faults, along with the most devastating earthquakes that have shaken the Indo-Gangetic basin.

### 3 MULTICHANNEL ANALYSIS OF SURFACE WAVES

Multichannel Analysis of Surface Waves (MASW) is a seismic surface wave geophysical method that records Rayleigh waves on a multichannel record. MASW has been widely used throughout the world for seismic site classification and site response studies. It consists of two methods viz. active survey and passive survey. The active MASW method generates surface waves actively through an impact source like a sledgehammer, whereas the passive method utilizes surface waves generated passively by cultural (e.g., traffic) or natural (e.g., thunder and tidal motion) activities. The entire process classically used to produce a  $V_s$  profile through spectral analysis of surface waves that involves three steps: acquisition of ground roll, construction of dispersion curve (a plot of phase velocity versus frequency), and back-calculation (inversion) of the  $V_s$  profile from the calculated dispersion curve.

For this study, active and passive surveys have been carried out at different locations in IGB using 2 Hz geophones. Test setup consists of 24 channel Geode seismograph in combination with 24 vertical geophones with the frequency of 2.0 Hz. An impulsive source of 15-pound sledgehammer striking against a 30 cm x 30 cm size steel plate generates surface waves, in the case of the active survey. However, to increase the investigation depth by several hundreds of meters, the high energy is needed to gain a few more Hz at the low-frequency end of a dispersion curve. Hence, passive surface waves generated from cultural (e.g., traffic) sources are usually of a low-frequency (1–30 Hz) nature with wavelengths ranging from a few km (natural sources) to a few tens (or hundreds) of meters (cultural sources), providing a wide range of penetration depths.

For obtaining the passive data, a passive roadside acquisition method by taking advantage of moving traffic for producing low frequency ambient noise. Park and Miller (2008) recommended that when performing a roadside surface wave survey using a linear receiver array, a 2-D dispersion analysis scheme that accounts for the offline nature of the passive surface waves need to be used. After acquiring the data using both active and passive MASW survey, the individual dispersion curves have been extracted from velocity– frequency diagram (typically shown as figure 2 (a)).

It is often useful or necessary to combine dispersion images processed from active and passive data sets for two reasons: (1) to enlarge the analyzable frequency (therefore depth) ranges of dispersion and (2) to better identify the modal nature of dispersion trends. Hence, combining the active and passive dispersion image has also studied to quantify the depth corresponding to both lower and upper frequency range. Figure 2 shows a typical dispersion curve and shear wave velocity profile for combined active and passive survey obtained from the field study.

### 4 DYNAMIC ROCK/SOIL MODEL

For representing the variation in small-strain soil/rock stiffness in the IGB, 75 profiles are used. Various researchers (Idriss, 1990; Boore et al., 1994 etc.) noted the significance of small-strain representation by shear modulus and shear wave velocity on the dynamic behavior of soil. As per Dobry et al. (2000), the complete characterization of small strain  $V_s$  from the ground surface down to the bedrock is often not economically feasible; the time-averaged  $V_s$  in the upper 30 m depth ( $V_{s30}$ ) has been adopted for seismic site classification. The value of  $V_{s30}$  is computed using

$$V_{s30} = \frac{30}{\sum_{i=1}^m \frac{H_i}{V_{Si}}} \quad [1]$$

where,  $H_i$ ,  $V_{Si}$  and  $m$  respectively represents the thickness of a layer  $i$ , shear wave velocity of layer  $i$  and number of layers in the top 30 m of soil. The sites have been classified as per National Hazard Reduction program (NEHRP, BSSC, 2003). Profiles with  $V_{s30} > 1500$  m/s,  $760 < V_{s30} \leq 1500$  m/s,  $360 < V_{s30} \leq 760$  m/s,  $180 < V_{s30} \leq 360$  m/s and  $V_{s30} < 180$  m/s respectively correspond to Site class A, B, C, D and E.

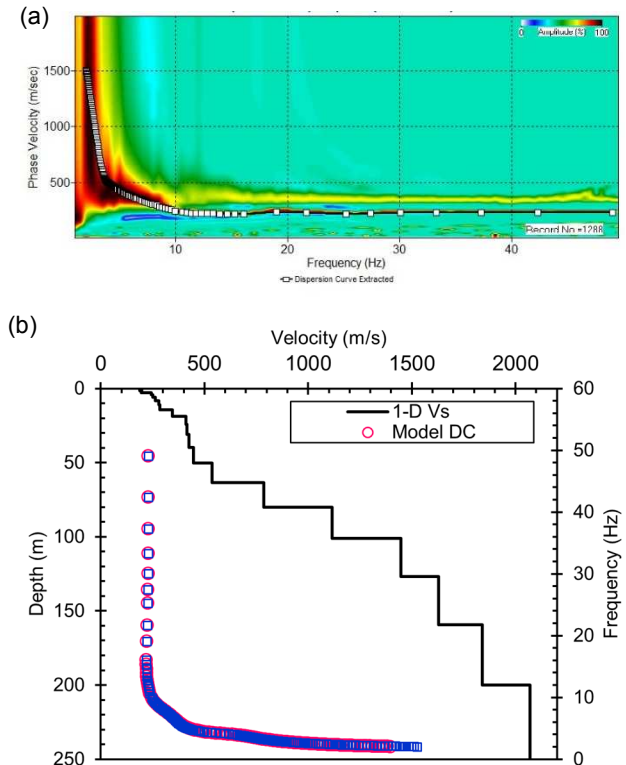


Figure 2. (a) Dispersion curve and (b) shear wave velocity obtained from combining active and passive survey using 2 Hz geophones

Out of 75 shear wave velocity profiles, around 60% is of site class C and D and 30% is of site class B and 10 % is of site class E. Figure 3 shows the representative shear

wave velocity profile for site class B, C, D and E obtained from the field study. Based on the statistical analysis of the different profiles it has been seen that average standard deviation ( $\sigma$ ) is in the range of 0.25-0.35 in the logarithm scale. Only the representative profiles are given in this paper, however, the profile comes with  $\pm \sigma$  of the representative profile has been used for site response study.

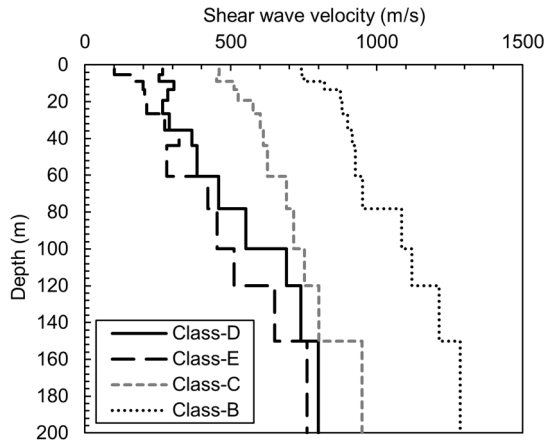


Figure 3. Typical shear wave velocity profile for site class grouped by NEHRP (BSSC, 2003) site class B, C, D and E

Over the years, several researchers have presented the different shear modulus and damping ratio values with shear strain for different materials. Out of all the available modulus reduction and damping curves for different soil types from existing literature, a set of curves are popularly used in the site response analysis. Widely used shear modulus and damping curves were developed by Seed and Idriss (1970), EPRI (1993), Vucetic and Dobry (1991), Ishibashi and Zhang (1993), Seed et al. (1986), Sun et al. (1988) and many more for representing the dynamic behaviour of the soil column. Hardin and Drnevich (1972), Kokusho (1980) and several other researchers recognized the effect of confining pressure on dynamic soil properties as the most significant for granular profiles.

In this study, the normalized shear modulus ( $G/G_{max}$ ) and material damping ratio ( $D$ ) developed by Zhang et al. (2005, 2008) has been used. Zhang et al. (2005) highlighted that strain ( $\gamma$ ), mean effective confining stress ( $\sigma'_m$ ), soil type and plasticity index (PI) are the most important factors that affect the ratio of shear modulus ( $G/G_{max}$ ). Sample  $G/G_{max}$  and  $D$  versus strain is given as Figure 4 for effective confining stress of 300 kPa and 1400 kPa for sand and clay (PI = 50%). For the half-space with  $V_{s30} \geq 760$  m/s, purely linear relationship for  $G/G_{max}$  and  $D$  is assumed as per Aboye et al. (2013)

## 5 GROUND MOTION DATABASE

The input ground motion is the prerequisite for any site response study. Hence, in this study, the ground motions are selected from both globally and locally available

recorded ground motion database. Globally recorded ground motion is taken from Pacific Earthquake Engineering Research database. Locally, recorded ground motions are collected from COSMOS (Consortium of Organization for Strong Motion Observation Systems) and PESMOS (Program for excellence in strong motion studies) database. All the recorded ground motions has been processed based on Boore (2005). The details regarding the processing these ground motions are also available in Bajaj et al. (2017).

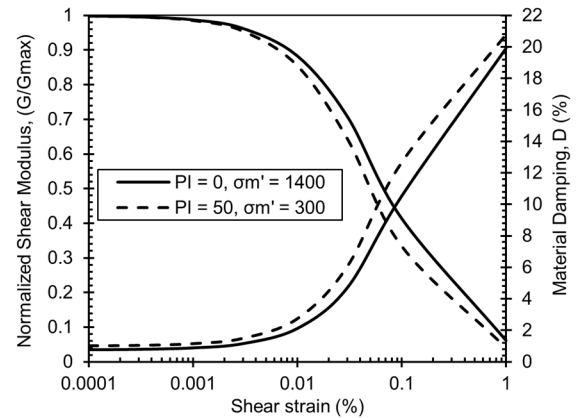


Figure 4. Sample  $G/G_{max}$  and  $D$  versus  $\gamma$  (Zhang et al., 2005)

For estimating the input ground motion, seismicity of the whole IGB has been studied. The whole area, shown in Figure 1 is divided into the grid size of  $0.5^\circ$  by  $0.5^\circ$ . Studying the local seismicity and developed probabilistic seismic hazard map around the site of measured shear wave velocity, it has concluded that hazard is dominated by the event with magnitude range ( $M_w$ ) from 6 to 9 and distance ( $R$ ) from 6 to 75 km. The range has been selected using the deaggregation of the seismic hazard for a return period of 2475 years. Hence the recorded ground motion is selected for a particular site considering local seismicity.

As the recorded ground motions for the Himalayan region are available only after 1986, hence the globally available strong motion database is also used to study the local site effect for the deep profiles in IGB. Recorded strong ground motions such as 1940 El-Centro, 1985 Mexico, 1989 Loma Prieta, 1994 Northridge, 1995 Hyogoken Nanbu and 1999 Chi-Chi etc. have been used in many of the site response studies in India. These ground motions were either used directly or scaled as per required peak ground acceleration (PGA) value. The other important factor while selecting the ground motions are its characteristics which controls the response of the soil column. These characteristics are frequency content, duration and amplitude of the ground motion. As local seismicity or seismic hazard analysis would only give the PGA at bedrock which would be only useful for determining amplitude while selecting ground motion. Therefore, seismicity alone would not be used for selecting the input ground motion for site response studies. Hence, in this study, the details regarding the fourier amplitude

spectrum (FAS) which corresponding source, site and path parameter has also studied, while selecting the ground motion. Based on Bajaj et al. (2017), the ground motion matches well with the region specific FAS and duration parameter has also considered in determining the local site effect. For a particular site, multiple ground motion are used for non-linear site response analysis. In that way uncertainty in the ground motion selection has reduced. Hence the ground motion for a site contains both near-site and far-site ground motions.

## 6 SITE RESPONSE ANALYSIS

Site response analysis is often used to estimate the ground motion characteristics at the surface of the soil column. For important projects, site-specific data is used to perform detailed site response analysis for the site, for which the wave propagation equation is solved for a particular site condition and ground motion. As the seismic waves pass through the soil deposit, site response can physically model the aspects of the wave propagation problem, unlike the other empirical studies, including effective stress models, pore water pressure generation, and dissipation models. In actual practice, only the one-dimensional (1D) wave propagation equation is usually solved as evident with the existence of various site response software such as Shake91, DEEPSOIL, EERA, STRATA.

The computer program DEEPSOIL (Hashash et al., 2016) is used to perform 1D total stress ground response analysis. The 1D assumption is taken to be valid for two reasons. First, because of subsequent refractions by the soil layers, stress waves propagate from the earthquake focus to the earth's surface in a nearly vertical path, especially close to the surface (Aboye et al., 2013). Second, soil properties generally vary more rapidly in the vertical direction than in the horizontal direction, making the vertical soil/rock column more important. The stated justifications are made by not taking the topography of the bedrock or earthquake directivity effects into account, which are not well established for IGB.

DEEPSOIL discretizes the entire 1D soil column into lumped multidegree of freedom elements with individual model parameters. The nonlinear behavior of soil is captured through the pressure dependent hyperbolic model for the backbone curve, developed by Konder and Zelasko (1963), modified by Matasovic (1993). The unloading and reloading formulations are based on the extended masing rules (Hashash et al., 2015).

The shear modulus reduction and damping curves were used to fit the modified hyperbolic model using the MRDF-UIUC procedure developed by Phillips and Hashash (2009). Many authors including, Hashash et al., (2010), have proposed modifications to the hyperbolic relationship to obtain a reasonable estimates of shear strength by post fitting the model. Hashash et al., (2016) proposes a generalized quadratic/hyperbolic strength controlled model to address this issue and the module has been implemented in DEEPSOIL. In this study, the formulation by Hashash et al. (2016) is used to obtain estimates of shear strength. Frequency independent rayleigh damping is used to model the small strain

damping as suggested by Phillips and Hashash (2009). Dependence of overburden pressure on the behavior of the modulus reduction curve and small strain damping is modeled through two coefficients in DEEPSOIL.

## 7 ASSESSMENT OF SITE AMPLIFICATION

Time histories obtained from ground response analyses can be used directly to represent ground surface motions. For determining the surface response, either synthetic time-histories can be derived to match the desired design ground surface response spectrum (U.S. Army Corps of Engineers 1999) or recorded motions can be scaled or modified to match the desired target spectrum. Generally, the direct use of response spectra calculated from the surface motions is not preferred in practice. However, it is advantageous and well accepted to obtain site amplification ratio from the ground response analyses. The site amplification factor is the ratio between equivalent measures of ground surface motion intensity and the intensity of corresponding input rock motion i.e.

$$AF = \frac{IM_{Soil}}{IM_{Rock}} \quad [2]$$

Where, IM and AF, respectively the intensity measure and amplification factor.

For the site response analysis of the deep IGB, firstly 2015, Nepal earthquake is given as the input time history at bedrock level, which is considered as the layer having  $V_{s30}$  760 m/s to determine the amplification factor for the representative site and given in Figure 3. The used input ground motion is recorded at KATNP station, which is at an epicentral distance of 59.9 km and the recorded PGA of 0.163 g. The variation of PGA value along the depth for all the representative sites is given as Figure 5. It can be seen that for site class E, amplification is more as compare to the other site class for the same ground motion.

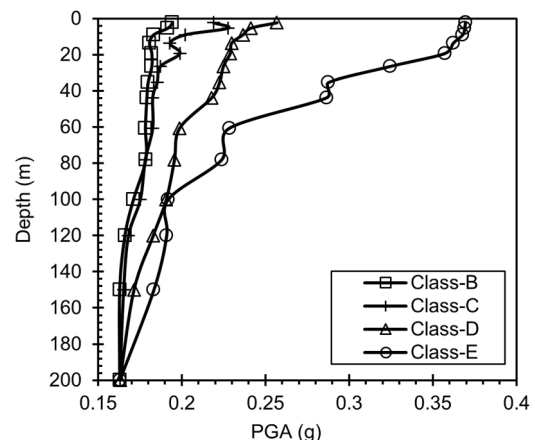


Figure 5. Variation of PGA value along the depth for Nepal, 2015 earthquake.

Variation of amplification factor with PGA value for different site class is also studied. As stated above, for a particular site, multiple ground motions are used based on

amplitude, frequency content and duration. Hence, variation of amplification factor with PGA is also studied. A typical example of variation of amplification factor with PGA for representative site class D (see Figure 3) is given as Figure 6. The variation amplification factors with PGA obtained from the present study is compared with the EPRI (1993), Ashford et al. (2000) and Kumar et al. (2016). It can be seen from Figure 6 that for lower PGA the outcome obtained from present study is matching well with the Kumar et al. (2016). A high value of amplification factor for low value of PGA is observed (See Figure 6). As per Romero and Rix (2005), large amplifications corresponding to low amplitude ground motions were observed during 1989 Loma Prieta EQ and 1985 Michoacan EQ. Large PGA are the attributes of large strains, hence, at large strains, the soil response is dominated by large damping values as observed from damping ratio versus strain plots of the soils. Due to large damping ratios, relatively low amplification factors are observed corresponding to input motions with large PGA.

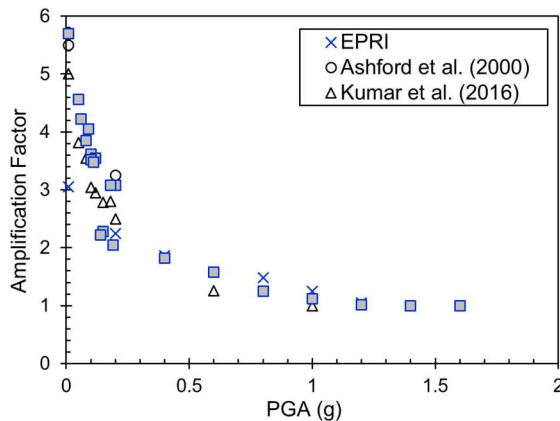


Figure 6. Variation of amplification factor with respect to PGA of different input ground motions

Further, all the shear wave velocity profiles are used for calculating the amplification factor. As explained above for a particular site different ground motion are used to put the variability in ground motion characteristics. A typical example of the variation of the amplification factor with depth for site class B is given as Figure 7. For all the sites that are classified as site class B, different input ground motions are used. In Figure 7, the mean of the amplification factor obtained by using 2015 Nepal earthquake ( $0.163g$ ,  $7.8M_w$ ,  $59.9$  km), 1999 ChiChi earthquake ( $0.183g$ ,  $7.6 M_w$ ,  $15.29$  km), 1979 Imperial Valley earthquake ( $0.169g$ ,  $6.5 M_w$ ,  $26.5$  km), 1994 Northridge earthquake ( $0.217g$ ,  $6.7 M_w$ ,  $26.8$  km) and 1966 Parkfield earthquake ( $0.357g$ ,  $6.1 M_w$ ,  $9.9$  km) applied to all the sites is also given. The solid black lines represent the mean of the amplification factor obtained from above mentioned strong ground motion. The light lines represent the mean of the amplification factor obtained at different site class by inputting the multiple ground motions. It can be seen from Figure 7 that different ground motions have different impact on the amplification factor. For example for the same sites, 2015

Nepal earthquake is giving different amplification factor than 1979 Imperial Valley earthquake. This is because of the change in the characteristic of the ground motion. Hence, from Figure 7, it can be concluded that for the determination of the amplification factor of the deep soil profiles, characteristic of the ground motion i.e. frequency content, duration and amplitude has a large impact on first 80 m of the soil column.

Based on the analysis, it has seen that for site class E, the range of amplification factor at the surface is 1.5 to 3.82 using randomly selected ground motions and from 2.35 to 7.58 using Site-specific ground motion as input. The used randomly selected ground motions have a similar distribution of amplitudes as of Site-specific ground motion. Similarly, a difference of around 30 to 35% is also observed in the case of site class D and C. Based on the analysis, it has determined that for the amplification range of site class E, D, C and B is 2.35 to 7.58, 1.82 to 5.58, 1.5 to 4.92 and 1.23 to 3.25 respectively in case of PGA.

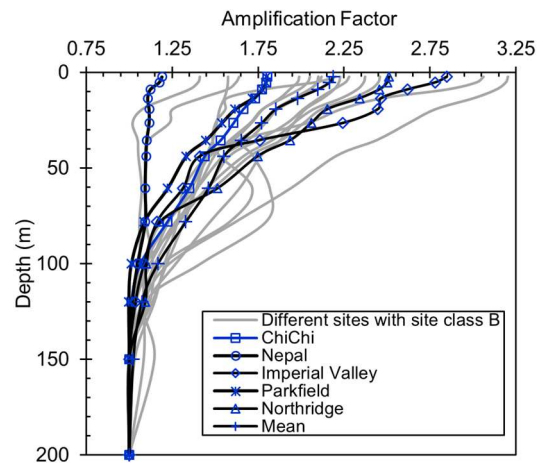


Figure 7. A typical example of the variation of the amplification factor with depth for site class B and comparing with the recorded ground motions

Further, the response spectra obtained from the site response analysis for different site at the surface is compared and dominant period has been studied. A typical example of the response spectra obtained at the surface and bedrock for site class B is given as Figure 8. The dotted grey lines represent the mean spectral acceleration (SA) at different period for different sites. The mean SA is calculated by using different input motion at the same site that is explained above. The solid blue and black line represents the mean SA at the bedrock and surface, these are further used for calculating the amplification factor corresponding to different sites.

Further, the amplification factor at different periods has been determined for different site class. The average amplification factor for the different site class is given as Figure 9. It has seen that for deep sites corresponding to site class B, C, D and E respectively amplified between the period 0.2 to 0.3 s, 0.8 to 1 s, 2 to 3 s and above 5 s.

## 8 CONCLUSION

Site response is indispensable as it controls the damage scenario during an earthquake. The extent of damages at any site is not only the function of earthquake magnitude and its distance from the epicentre but also the subsoil characteristics at the site. The response of shallow and deep soil columns is also different for the same intensity of earthquakes. In this study, an attempt has been made to determine the amplification factor of the deep soil sites in the Indo Gangetic Basin. Firstly, the shear wave velocity up to 200 m depth has been determined based on the geophysical test named multichannel analysis of the shear wave. Further, these sites were classified based on time-averaged  $V_s$  in the upper 30 m depth as per NEHRP (BSSC,2003). The obtained  $V_s$  profiles were further used to estimate the site-specific response parameters at different locations by carrying out non-linear site response analysis. The input ground motions for site response analysis selected considering seismicity and availability. Based on the analysis, it was seen that for site class E, the range of amplification factor at the surface is 1.5 to 3.82 using randomly selected ground motions and from 2.35 to 7.58 using Site-specific ground motion as input. Similarly, difference of around 30 to 35% is also observed in case of site class D and C. Based on the analysis, it has determined that for the amplification range of site class E, D, C and B is 2.35 to 7.58, 1.82 to 5.58, 1.5 to 4.92 and 1.23 to 3.25 respectively.

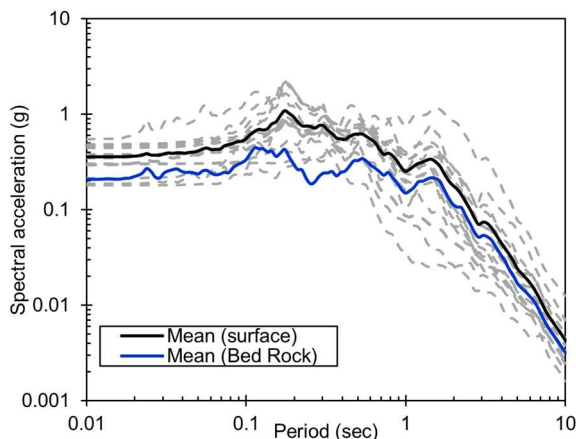


Figure 8. A typical example of the response spectra for site class B showing its mean at the surface and bedrock.

## 9 ACKNOWLEDGEMENT

The authors would like to thank the Science and Engineering Research Board (SERB) of the Department of Science and Technology (DST), India for funding the project titled "Measurement of shear wave velocity at deep soil sites and site response studies", Ref: SERB/F/162/2015-2016.

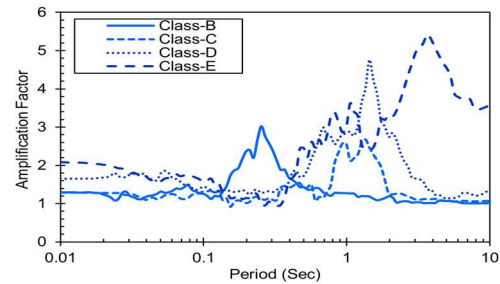


Figure 9. Showing the comparison of amplification factor for different spectral period for seismic site class B, C, D and E

## 10 REFERENCES

- Aboye S., 2013. Seismic Site Coefficient Model and Improved Design Response Spectra Based on Conditions in South Carolina, Ph.D. Dissertation, Clemson University, Clemson SC, 281 pp.
- Anbazhagan P., Sitharam T.G., 2008. Spatial variability of the weathered and engineering bedrock using multichannel analysis of surface wave survey. *Pure Appl Geophys* 166(3):409–428.
- Anbazhagan P., Kumar A., Sitharam T.G., 2010. Amplification factor from intensity map and site response analysis for the soil sites during 1999 Chamoli earthquake. In: Proceedings of the 3rd Indian young geotechnical engineers conference, New Delhi pp 311–316
- Ashford S.A., Warrasak J., Panitan L., 2000. Amplification of Earthquake Ground Motions in Bangkok. In: Proceedings of 12th world conference on earthquake engineering 1466
- Bajaj K., Anbazhagan P., Moustafa S. S. R. and Al-Arifi N. S. N., 2017. Attenuation characterization of the Himalayan region using spectral analysis of seismic waves, *Bulletin of seismology society of America* (Under review)
- Boominathan A., Dodagoudar G.R., Suganthi A, Maheshwari R.U., 2008. Seismic hazard assessment of Chennai city considering local site effects. *J Earth Syst Sci* 117(S2):853–863
- Bilham R. and Ambraseys N., 2005. Apparent Himalayan slip deficit from the summation of seismic moments for Himalayan earthquakes, 1500–2000. *Curr Sci* 88: 1658–1667
- Bilham R et al., 2001. Himalayan seismic hazard, *Science* 293: 1442–1444
- Boore, D.M., Joyner, W.B., and Fumal, T.E., 1994. Estimation of Response Spectra and Peak Acceleration from Western North American Earthquakes: An Interim Report, *USGS Open-File Rep. 93-509*, vol. 2, U.S. Geological Survey (USGS), 94–124.
- Boore, D. M., 2012. SMSIM, software, [http://www.daveboore.com/software\\_online.html](http://www.daveboore.com/software_online.html).
- Boore, D. M., 2005. On pads and filters: Processing strong-motion data, *Bull. Seism. Soc. Am.* 95: 745–750.
- BSSC (2003) NEHRP recommended provision for seismic regulation for new buildings and other structures



- (FEMA 450). Part 1: provisions, building safety seismic council for the federal Emergency Management Agency, Washington DC
- Chapman, M. C., Martin, J. R., Olgun, C. G., and Beale, J. N., 2006. Site-response models for Charleston, South Carolina and vicinity developed from shallow geotechnical investigations, *Bulletin of the Seismological Society of America* 96, 467–489.
- COSMOS (Consortium of Organization for Strong Motion Observation Systems) <http://www.strongmotioncenter.org/vdc/scripts/default.plx> (last accessed 31 January 2017)
- Desai S.S. and Choudhury D., 2014. Spatial variation of probabilistic seismic hazard of Mumbai and surrounding region. *Nat Hazards* 17(1):1873–1898
- Desai S.S. and Choudhury D., 2015. Site-specific seismic ground response study for Nuclear power plants and ports in Mumbai. *Nat Hazards Rev.* doi:10.1061/(ASCE)NH.15276996.0000177,04015002
- Dobry, R., Borcherdt, R.D., Crouse, C.B., Idriss, I.M., Joyner, W.B., Martin, G.R., Power, M.S., Rinne, E.E., and Seed, R.B., 2000. New site coefficients and site classification system used in recent building seismic code provisions, *Earthquake Spectra* 16:41–67.
- Electric Power Research Institute (EPRI) 1993, Guidelines for Site-specific Ground Motions, Palo Alto, California, November, TR-102293.
- Gupta, I.D, 2006, Delineation of probable seismic sources in India and neighbourhood by a comprehensive analysis of seismotectonic characteristics of the region, *Soil Dynamics and Earthquake Engineering*, 26: 766–790.
- Hardin B.O. and Drnevich V.P. 1972. Shear modulus and damping in soils: design equations and curves, *Soil Mechanics and Foundation Division*, ASCE, 98(7), 667-692.
- Hashash Y.M.A and Park D. 2001, Non-linear one-dimensional seismic ground motion propagation in the Mississippi embayment, *Engineering Geology*, 62(1–3): 185–206.
- Hashash, Y. M. A., C. Phillips and D.R. Groholski, 2010. Recent advances in non-linear site response analysis. Fifth International Conference in Recent Advances in Geotechnical Earthquake Engineering and Soil Dynamics. San Diego, CA. CD-Volume: OSP 4.
- Hashash Y M A, Musgrove M I, Harmon J A, Groholski D R, Phillips C A and Park D. 2016, DEEPSOIL 6.1, User Manual, Urbana, IL, Board of Trustees of University of Illinois at Urbana-Champaign.
- Ishibashi I and Zhang X. 1993, Unified dynamic shear moduli and damping ratios of sand and clay. *Soils and Foundations*, 33(1): 182-191.
- Idriss, I. M., 1990. Response of soft soil sites during earthquake, in H. Bolton Seed: Memorial Symposium Proceedings, vol. 2, BiTech Publishers, Richmond, BC, 273–289.
- Kokusho T. 1980. Cyclic triaxial test of dynamic soil properties for wide strain range. *Soils and Foundations*, 20: 45-60.
- Kondner, R. L., and Zelasko, J. S., Hyperbolic stress-strain formulation of sands. Second pan American Conference on Soil Mechanics and Foundation Engineering, Sao Paulo, Brazil, 289-324.
- Kumar A., Anbazhagan P., Sitharam T.G., 2012. Site-specific ground response study of deep Indo-Gangetic Basin Using representative regional ground motions, Geo-Congress, State of art and practice in Geotechnical Engineering, Oakland California, paper no. 1065
- Kumar A., Bora O., Harinarayan N.H., 2016. Obtaining the surface PGA from site response based on globally recorded ground motions and matching with the codal values. *Nat Hazards*, 81:543-572.
- Matasovic, N. 1993. Seismic response of composite horizontally-layered soil deposits Ph.D. Thesis, University of California, Los Angeles.
- PESMOS (Program for excellence in strong motion studies), <http://pesmos.in/2011/> (last accessed 31 January 2017).
- Phillips, C. and Y.M.A. Hashash 2009. Damping formulation for non-linear 1D site response analyses. *Soil Dynamics and Earthquake Engineering* 29(7): 1143-1158.
- Park C. B. and Miller R. D., 2008. Roadside Passive Multichannel Analysis of Surface Waves (MASW). *Journal of Environmental and Engineering, Geophysics*, 13: 1-11
- Rao M.B.R., 1973. The subsurface geology of the IndoGangetic plains, *J. Geol. Soc. India*, 14:217–242.
- Romero SM, Rix GJ, 2005. Ground motion amplification of soils in the upper Mississippi embayment. Report no. GIT-CEE/GEO-01-1, National Science Foundation Mid America Earthquake Center
- Singh I.B., 1996. Geological evolution of Ganga plain-An overview. *Journal of the Palaeontological society of India*, 41: 99-137
- Seed H.B. and Idriss I.M., 1970, Soil moduli and damping factors for dynamic response analyses. Technical Report EERC-70-10, University of California, Berkeley.
- Seed H., Wong R., Idriss I. and Tokimatsu K.. 1986. Moduli and Damping Factors for Dynamic Analyses of Cohesionless Soils. *Journal of Geotechnical Engineering*, 112(11): 1016–1032.
- Sun J.I., Golesorkhi R. and Seed H.B. 1988. Dynamic moduli and damping ratios for cohesive soils. EERC Report No. UCB/EERC-88/15.
- U.S. Army Corps of Engineers, 1999. Engineer manual, EM1110-2-6050, engineering and design: response spectra and seismic analysis for concrete hydraulic structures, 30 June 1999, Washington, DC 20314-1000
- Vucetic M and Dobry R. 1991. Effect of Soil Plasticity on Cyclic Response. *Journal of Geotechnical Engineering*, 117(1): 89–107.
- Zhang, J., Andrus, R.D., and Juang, C.H., 2005. Normalized shear modulus and material damping ratio relationships, *Journal of Geotechnical and Geoenvironmental Engineering* 131: 453–464.
- Zhang, J., Andrus, R.D., and Juang, C.H., 2008. Model uncertainty in normalized shear modulus and damping relationships, *Journal of Geotechnical and Geoenvironmental Engineering* 134: 24–36.